Supplementary Information

Conformational dynamics of deubiquitinase A and the functional implications

Ashish Kabra and Ying Li*

Department of Chemistry, University of Louisville, Louisville, KY 40208

E-mail: ying.li.1@louisville.edu

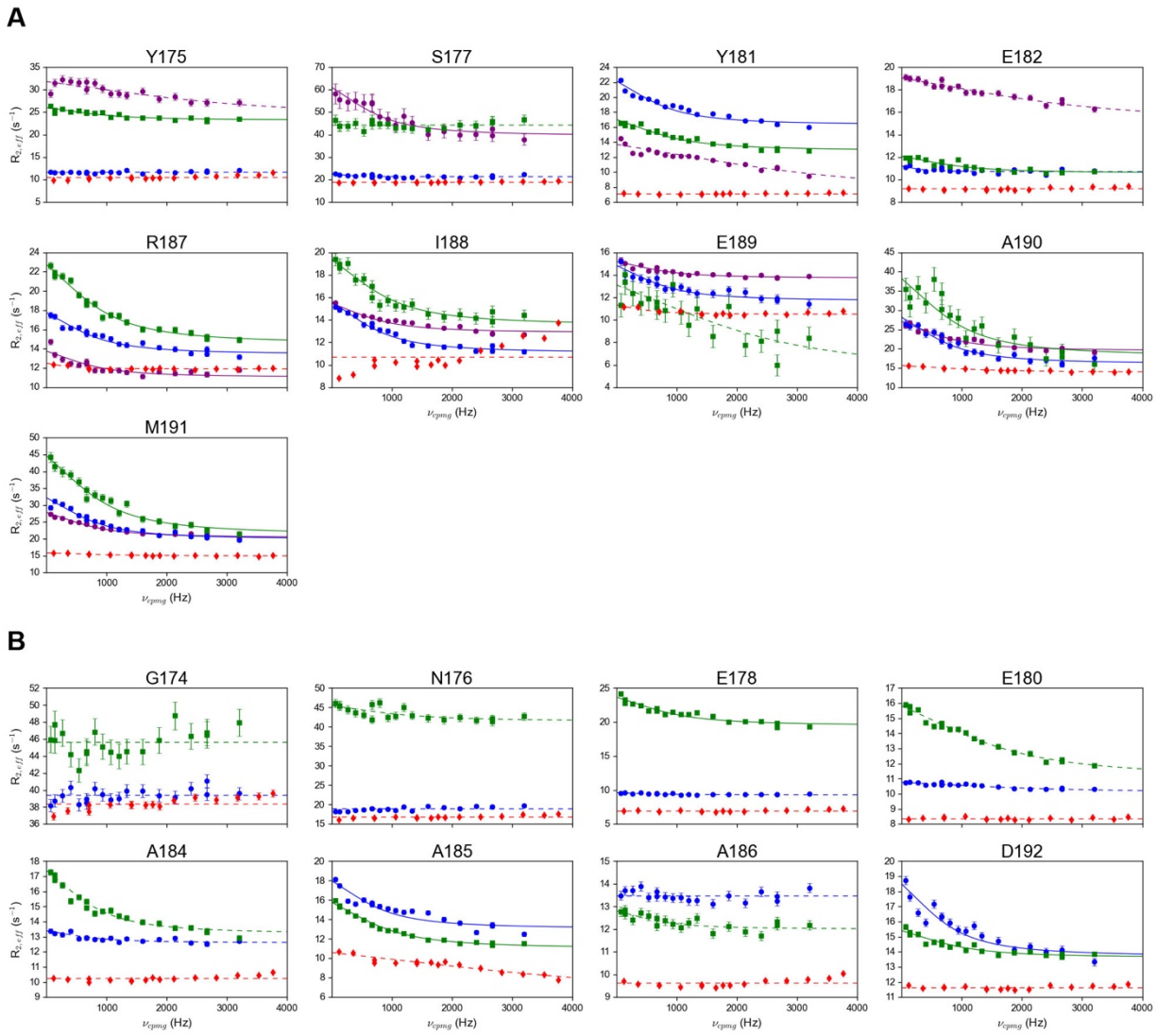

Figure S1. The amide ^{1}H relaxation dispersion profiles of all assigned residues N-terminal to the α2 helix (residues 174-192) in wild-type p-DUBA (purple circle for **a** conformer; blue circle for **b** conformer or the only conformer), wild-type np-DUBA (green square), and p-R272E/K273E mutant (red diamond). Residues showing two conformers are displayed in panel A and residues showing only one conformer are displayed in panel B. The dashed lines indicate individual fits and the solid lines indicate group fits. Residues that display less than 35% uncertainty in k_{ex} in individual fitting and satisfy $\chi^2_{group}/\chi^2_{invididual} < 2.0$ were group fit. The data were acquired at 298 K and 700 MHz ^{1}H frequency.

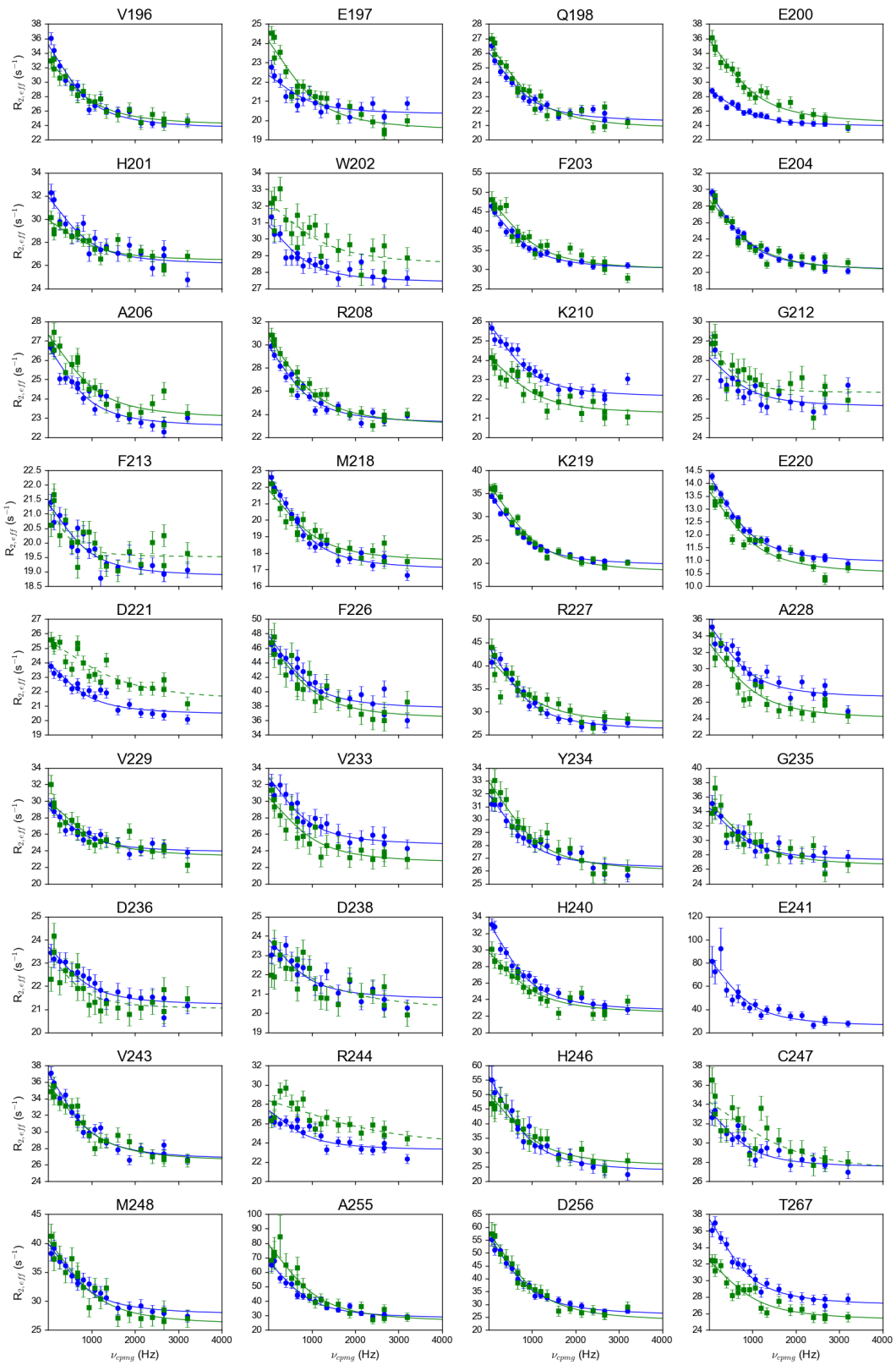

(figure continued on the next page)

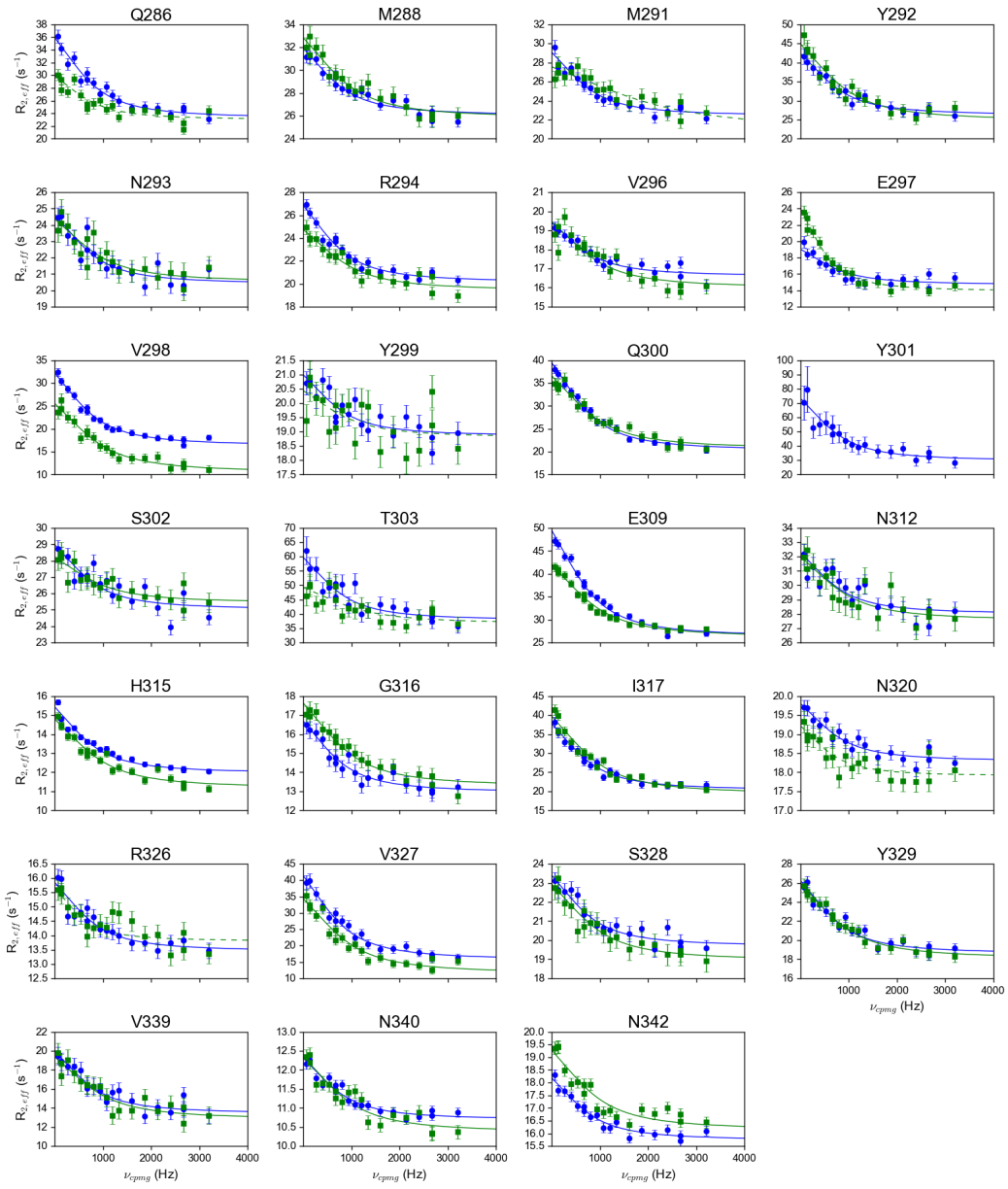

Figure S2. The amide ^{1}H relaxation dispersion profiles of wild-type p-DUBA (blue) and np-DUBA (green). Only residues C-terminal to the α1-α2 loop and were group fit in p-DUBA are displayed. The solid lines indicate group fits and the dashed lines indicate individual fits. Residues that display less than 35% uncertainty in k_{ex} in individual fitting and satisfy $\chi^2_{group}/\chi^2_{invididual} < 2.0$ were group fit. Other residues were fit individually. The data were acquired at 298 K and 700 MHz ^{1}H frequency.

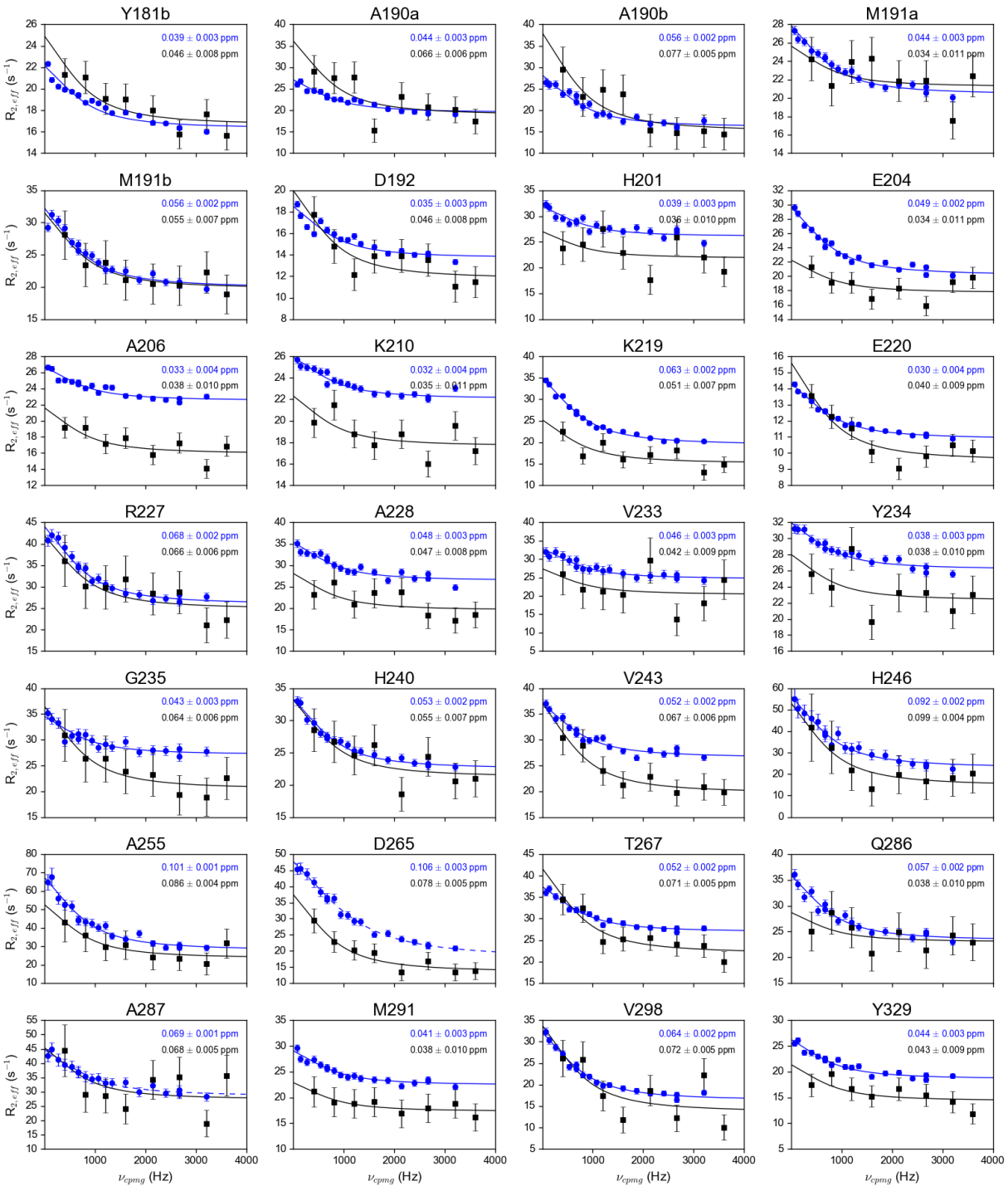

Figure S3. Representative amide ^{1}H relaxation dispersion profiles of wild-type p-DUBA measured at 580 μM (blue) and 100 μM (black) protein concentrations. The data on the low concentration sample was fit with k_{ex} set to 4954 s^{-1}, which is the rate constant determined from the high concentration sample; other parameters were unconstrained. The solid lines indicate group fits and the dashed lines indicate individual fits. The $\boldsymbol{\phi_{ex}^{1/2}}$ values for both samples are displayed in each panel.

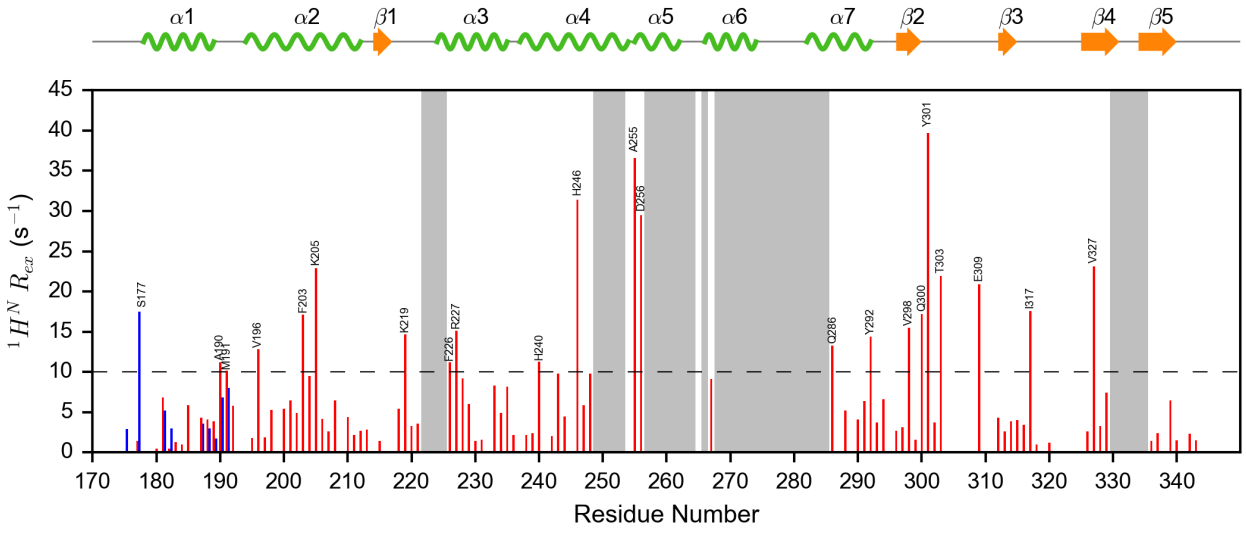

Figure S4. R_{ex} of 101 residues showing conformational exchange in p-DUBA. R_{ex} was estimated from the differences in $R_{2,eff}$ at ν_{cpmg} = 66.7 Hz and 3200 Hz. The blue bars represent the **a** conformer; the red bars represent the **b** conformer or the only conformer. The dashed line indicates 10 s^{-1}. For residues with R_{ex} >10 s^{-1}, the residue names and numbers are displayed above the bars. The regions shaded in grey represent non-proline residues without detectable NMR signals. The secondary structure derived from the crystal structure of DUBA (PDB code: 3TMP) is displayed above the plot. The data were acquired at 298 K and 700 MHz ^{1}H frequency.

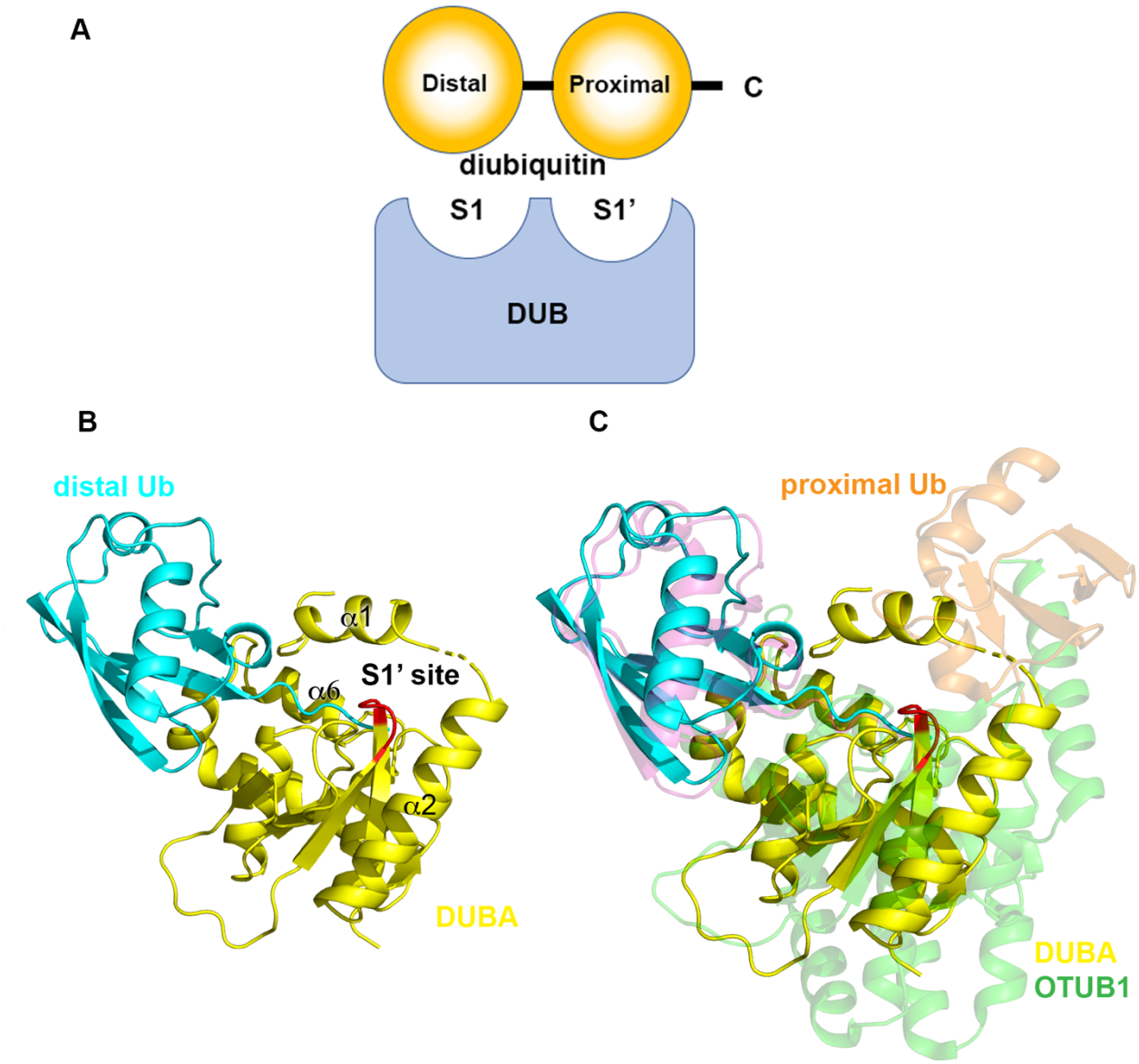

Figure S5. (A) Nomenclature used to identify binding sites on DUBs and to name the ubiquitin unit within the diubiquitin molecule. (B) The crystal structure of DUBA conjugated to the ubiquitin(Ub) aldehyde (PDB code: 3TMP) with the S1' site deduced from the crystal structure of h/ceOTUB1-Ub aldehyde-UBC13~Ub (PDB code: 4DHZ).[1] The His loop is highlighted in red. (C) The crystal structure of h/ceOTUB1 (PDB code: 4DHZ) with the bound distal and proximal ubiquitins superimposed to the crystal structure of DUBA (PDB code: 3TMP).

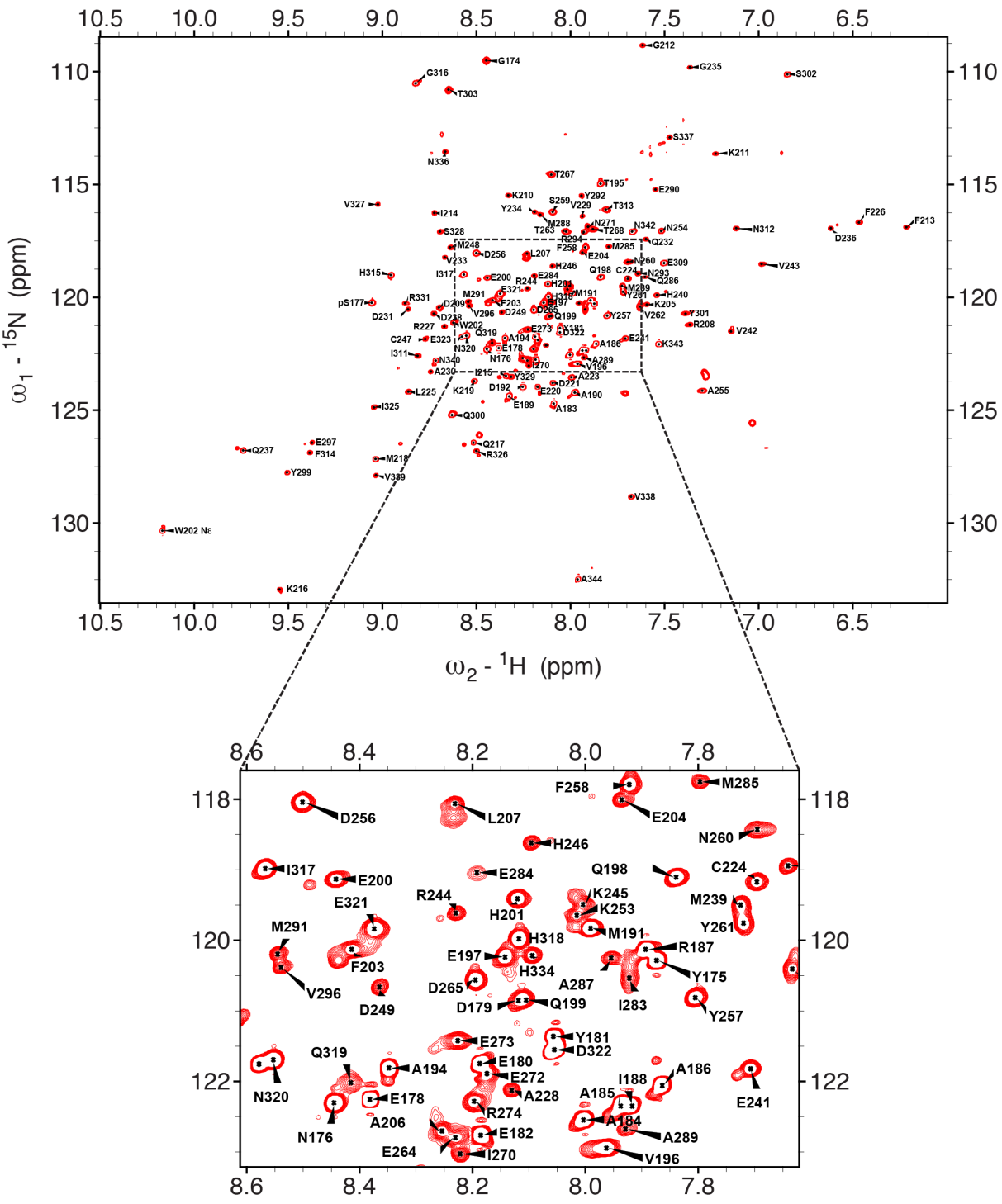

Figure S6. ^{15}N TROSY spectrum of p-R272E/K273E mutant with assignments labeled. The data were acquired at 300 K and 700 MHz 1H frequency.

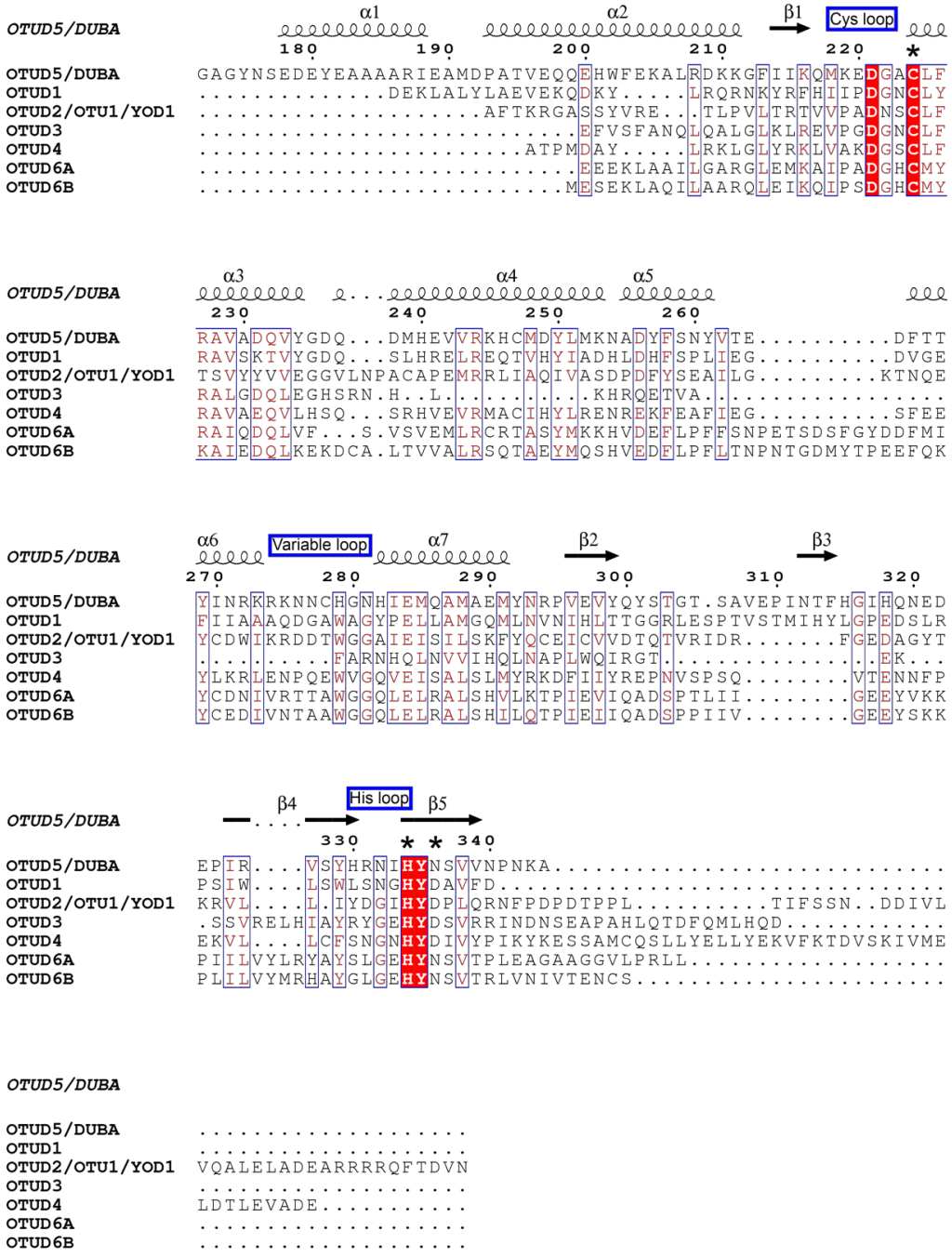

Figure S7. Alignment of amino acid sequences of the catalytic domains of OTU DUBs with small catalytic domains. The fully conserved residues are shaded in red. Blue box indicates residues displaying higher than 70% similarities. The asterisks indicate the catalytic residues. The secondary structure of OTUD5/DUBA from the crystal structure (PDB code: 3TMP) is displayed above the sequences. Sequence alignment was performed using Clustal Omega.[2] The sequence similarities and secondary structure were rendered with ESPript.[3]

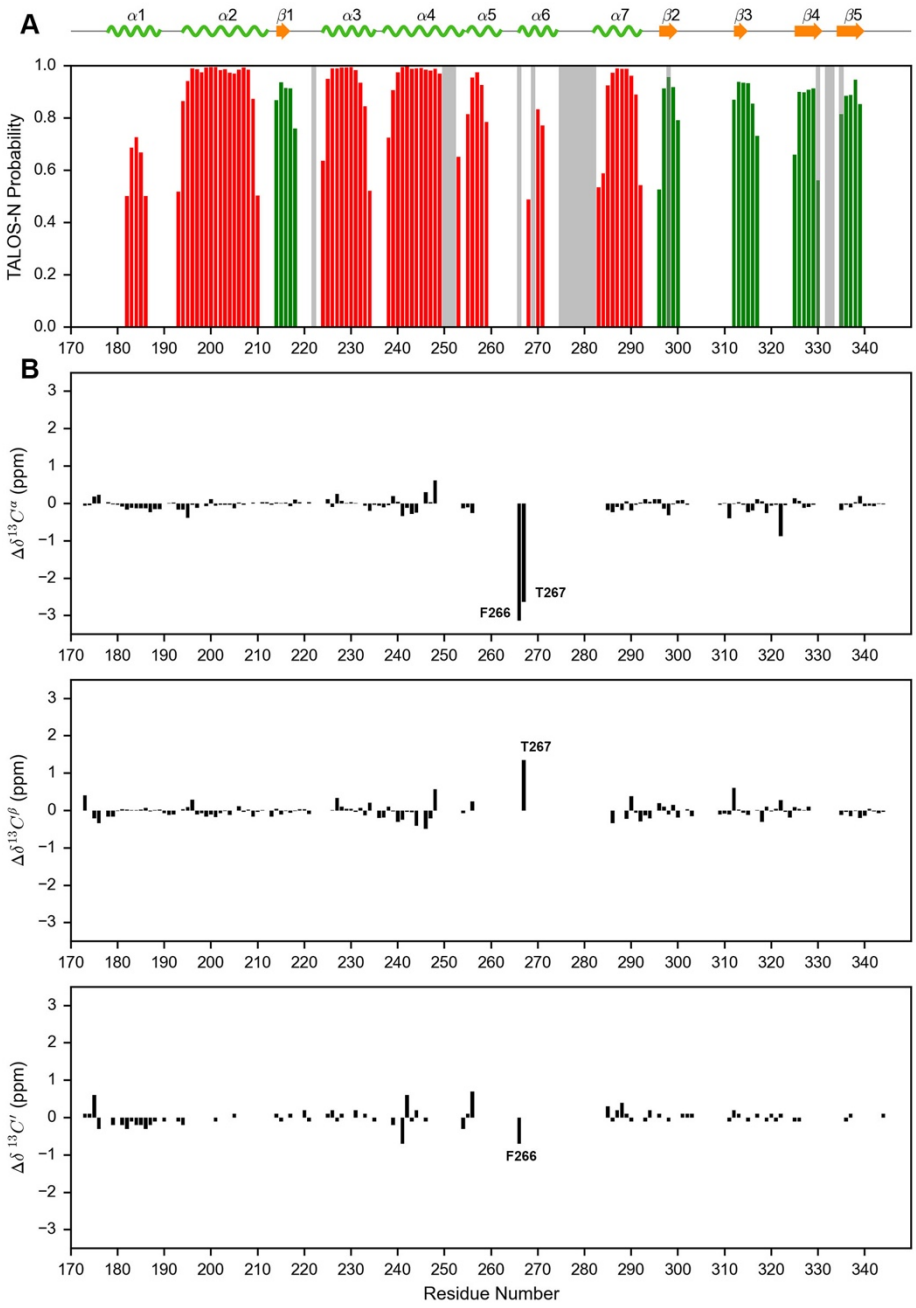

Figure S8. (A) Secondary structure of the R272E/K273E mutant predicted from $^{1}H^{N}$, ^{15}N, $^{13}C^{\alpha}$, $^{13}C^{\beta}$ and $^{13}C'$ by TALOS-N.[4] Alpha helices are represented by red bars and beta strands are represented by green bars. Invisible residues are shaded in grey. (B) $^{13}C^{\alpha}$, $^{13}C^{\beta}$ and $^{13}C'$ chemical shift differences between the R272E/K273E mutant and the wild-type. The secondary structure derived from the crystal structure of p-DUBA conjugated to ubiquitin-aldehyde (PDB code: 3TMP) is displayed above the plots.

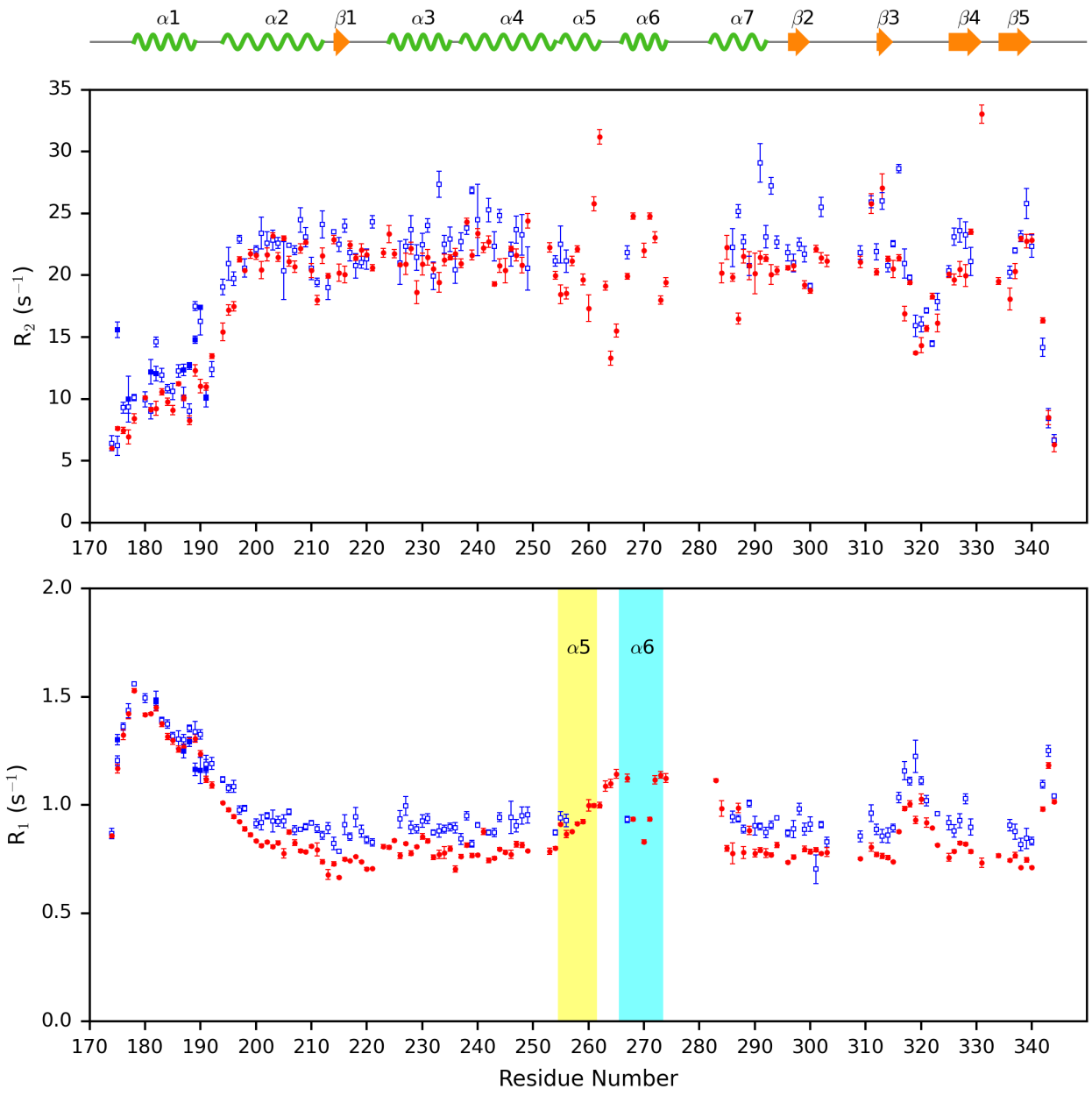

Figure S9. Comparison of ^{15}N R_1 and R_2 relaxation rates of wild-type p-DUBA (blue) and p-R272E/K273E mutant (red). The closed squares represent the **a** conformer and the open squares represent the **b** conformer or the only conformer in p-DUBA. The α5 and α6 helices were shaded in yellow and cyan, respectively, in the R_1 plot. The secondary structure derived from the crystal structure of p-DUBA conjugated to ubiquitin-aldehyde (PDB code: 3TMP) is displayed above the plots. The data were acquired at 298 K and 700 MHz ^1H frequency. The data on p-R272E/K273E were deposited into the BMRB under the accession code 50686.

Table S1. Group fits of R_2 relaxation dispersion curves of p-DUBA

Name	R_{ex} (s^{-1})	$\boldsymbol{\phi_{ex}^{1/2}}$(ppm)	Name	R_{ex} (s^{-1})	$\boldsymbol{\phi_{ex}^{1/2}}$(ppm)	k_{ex} (s^{-1})
S177a	21.6 ± 0.4	0.074 ± 0.002	D238	3.1 ± 0.4	0.028 ± 0.004	4954 ± 82
Y181b	5.8 ± 0.4	0.039 ± 0.003	H240	10.8 ± 0.4	0.053 ± 0.002	
A183	1.7 ± 0.4	0.021 ± 0.006	E241	58.7 ± 0.5	0.123 ± 0.001	
A185	4.9 ± 0.4	0.035 ± 0.003	V243	10.5 ± 0.4	0.052 ± 0.002	
R187a	2.7 ± 0.4	0.026 ± 0.005	R244	4.1 ± 0.4	0.033 ± 0.004	
R187b	4.3 ± 0.4	0.033 ± 0.004	H246	33.3 ± 0.4	0.092 ± 0.001	
I188a	2.6 ± 0.4	0.026 ± 0.005	C247	5.9 ± 0.4	0.039 ± 0.003	
I188b	4.5 ± 0.4	0.034 ± 0.003	M248	12.3 ± 0.4	0.056 ± 0.002	
E189a	1.5 ± 0.4	0.019 ± 0.006	A255	39.4 ± 0.4	0.100 ± 0.001	
E189b	3.1 ± 0.4	0.028 ± 0.004	D256	30.8 ± 0.4	0.089 ± 0.002	
A190a	7.6 ± 0.4	0.044 ± 0.003	T267	10.5 ± 0.4	0.052 ± 0.002	
A190b	12.1 ± 0.4	0.056 ± 0.002	Q286	12.6 ± 0.4	0.057 ± 0.002	
M191a	7.4 ± 0.4	0.044 ± 0.003	M288	5.9 ± 0.4	0.039 ± 0.003	
M191b	12.3 ± 0.4	0.056 ± 0.002	M291	6.6 ± 0.4	0.041 ± 0.003	
D192	4.8 ± 0.4	0.035 ± 0.003	Y292	16.2 ± 0.4	0.064 ± 0.002	
V196	11.6 ± 0.4	0.055 ± 0.002	N293	4.2 ± 0.4	0.033 ± 0.004	
E197	2.0 ± 0.4	0.023 ± 0.005	R294	6.7 ± 0.4	0.041 ± 0.003	
Q198	4.8 ± 0.4	0.035 ± 0.003	V296	2.8 ± 0.4	0.027 ± 0.004	
E200	5.1 ± 0.4	0.036 ± 0.003	E297	4.4 ± 0.4	0.033 ± 0.004	
H201	5.9 ± 0.4	0.039 ± 0.003	V298	15.8 ± 0.4	0.064 ± 0.002	
W202	3.5 ± 0.4	0.030 ± 0.004	Y299	2.1 ± 0.4	0.023 ± 0.005	
F203	16.6 ± 0.4	0.065 ± 0.002	Q300	19.1 ± 0.4	0.070 ± 0.002	
E204	9.5 ± 0.4	0.049 ± 0.002	Y301	43.7 ± 0.5	0.106 ± 0.001	
A206	4.2 ± 0.4	0.033 ± 0.004	S302	3.9 ± 0.4	0.032 ± 0.004	
R208	6.7 ± 0.4	0.041 ± 0.003	T303	21.9 ± 0.4	0.075 ± 0.002	
K210	3.9 ± 0.4	0.031 ± 0.004	E309	23.1 ± 0.4	0.077 ± 0.002	
G212	2.6 ± 0.4	0.026 ± 0.005	N312	4.3 ± 0.4	0.033 ± 0.004	
F213	2.5 ± 0.4	0.025 ± 0.005	H315	3.5 ± 0.4	0.030 ± 0.004	
M218	5.8 ± 0.4	0.039 ± 0.003	G316	3.7 ± 0.4	0.031 ± 0.004	
K219	15.6 ± 0.4	0.063 ± 0.002	I317	17.3 ± 0.4	0.067 ± 0.002	
E220	3.4 ± 0.4	0.030 ± 0.004	N320	1.5 ± 0.4	0.020 ± 0.006	
D221	3.6 ± 0.4	0.030 ± 0.004	R326	2.4 ± 0.4	0.025 ± 0.005	
F226	10.2 ± 0.4	0.051 ± 0.002	V327	25.7 ± 0.4	0.081 ± 0.002	
R227	18.0 ± 0.4	0.068 ± 0.002	S328	3.7 ± 0.4	0.031 ± 0.004	
A228	8.9 ± 0.4	0.048 ± 0.003	Y329	7.7 ± 0.4	0.044 ± 0.003	
V229	5.4 ± 0.4	0.037 ± 0.003	V339	6.5 ± 0.4	0.041 ± 0.003	
V233	8.3 ± 0.4	0.046 ± 0.003	N340	1.6 ± 0.4	0.020 ± 0.006	
Y234	5.8 ± 0.4	0.039 ± 0.003	N342	2.4 ± 0.4	0.025 ± 0.005	
G235	7.4 ± 0.4	0.043 ± 0.003				
D236	2.5 ± 0.4	0.026 ± 0.005				

Table S2. Group fits of R_2 relaxation dispersion curves of np-DUBA

Name	R_{ex} (s^{-1})	$\boldsymbol{\phi_{ex}^{1/2}}$(ppm)	Name	R_{ex} (s^{-1})	$\boldsymbol{\phi_{ex}^{1/2}}$(ppm)	k_{ex} (s^{-1})
Y175	2.8 ± 0.5	0.029 ± 0.005	M248	14.8 ± 0.5	0.066 ± 0.002	5750 ± 110
E178	4.2 ± 0.5	0.035 ± 0.004	D249	31.2 ± 0.5	0.096 ± 0.002	
Y181	4.1 ± 0.5	0.035 ± 0.004	A255	54.1 ± 0.6	0.127 ± 0.002	
E182	1.5 ± 0.5	0.021 ± 0.006	D256	35.0 ± 0.5	0.102 ± 0.002	
A183	1.3 ± 0.5	0.020 ± 0.007	T267	7.3 ± 0.5	0.047 ± 0.003	
A185	4.7 ± 0.5	0.038 ± 0.004	M288	7.0 ± 0.5	0.046 ± 0.003	
R187	8.2 ± 0.5	0.049 ± 0.003	E290	12.5 ± 0.5	0.061 ± 0.002	
I188	5.8 ± 0.5	0.042 ± 0.003	Y292	20.0 ± 0.5	0.077 ± 0.002	
A190	20.1 ± 0.5	0.077 ± 0.002	N293	3.8 ± 0.5	0.034 ± 0.004	
M191	23.3 ± 0.5	0.083 ± 0.002	R294	5.3 ± 0.5	0.040 ± 0.003	
D192	1.8 ± 0.5	0.023 ± 0.006	V296	3.5 ± 0.5	0.032 ± 0.004	
T195	3.8 ± 0.5	0.033 ± 0.004	V298	15.0 ± 0.5	0.067 ± 0.002	
V196	9.0 ± 0.5	0.052 ± 0.003	Q300	15.9 ± 0.5	0.069 ± 0.002	
E197	4.7 ± 0.5	0.037 ± 0.004	S302	2.8 ± 0.5	0.029 ± 0.005	
Q198	6.0 ± 0.5	0.042 ± 0.003	E309	15.7 ± 0.5	0.068 ± 0.002	
E200	11.7 ± 0.5	0.059 ± 0.002	N312	4.5 ± 0.5	0.037 ± 0.004	
H201	3.6 ± 0.5	0.033 ± 0.004	T313	4.6 ± 0.5	0.037 ± 0.004	
F203	18.8 ± 0.5	0.075 ± 0.002	F314	3.9 ± 0.5	0.034 ± 0.004	
E204	8.7 ± 0.5	0.051 ± 0.003	H315	3.6 ± 0.5	0.033 ± 0.004	
K205	21.7 ± 0.5	0.081 ± 0.002	G316	4.4 ± 0.5	0.036 ± 0.004	
A206	4.4 ± 0.5	0.036 ± 0.004	I317	20.3 ± 0.5	0.078 ± 0.002	
R208	7.7 ± 0.5	0.048 ± 0.003	V327	22.8 ± 0.5	0.082 ± 0.002	
K210	3.0 ± 0.5	0.030 ± 0.004	S328	4.0 ± 0.5	0.034 ± 0.004	
I215	1.9 ± 0.5	0.024 ± 0.006	Y329	7.8 ± 0.5	0.048 ± 0.003	
M218	4.4 ± 0.5	0.036 ± 0.004	V339	6.5 ± 0.5	0.044 ± 0.003	
K219	19.4 ± 0.5	0.076 ± 0.002	N340	2.0 ± 0.5	0.024 ± 0.006	
E220	3.2 ± 0.5	0.031 ± 0.004	N342	3.1 ± 0.5	0.031 ± 0.004	
F226	10.7 ± 0.5	0.056 ± 0.002				
R227	14.3 ± 0.5	0.065 ± 0.002				
A228	9.2 ± 0.5	0.052 ± 0.003				
V229	6.9 ± 0.5	0.045 ± 0.003				
V233	8.0 ± 0.5	0.049 ± 0.003				
Y234	7.1 ± 0.5	0.046 ± 0.003				
G235	8.9 ± 0.5	0.051 ± 0.003				
H240	7.4 ± 0.5	0.047 ± 0.003				
V243	9.4 ± 0.5	0.053 ± 0.003				
H246	25.3 ± 0.5	0.087 ± 0.002				

Table S3. Individual fits of R_2 relaxation dispersion curves of p-R272E/K273E*

Name	k_{ex} (s^{-1})	R_{ex} (s^{-1})	$\phi_{ex}^{1/2}$(ppm)	Name	k_{ex} (s^{-1})	R_{ex} (s^{-1})	$\phi_{ex}^{1/2}$(ppm)
A190	7700± 920	1.74±0.07	0.026±0.002	T263	18700±2400	13± 1	0.11±0.01
T195	1790± 600	1.31±0.04	0.011±0.001	D265	7590± 600	2.64±0.07	0.032±0.001
V196	10800±1500	3.1±0.2	0.041±0.004	T267	20000±3300	14± 2	0.12±0.02
E197	3500±1100	1.61±0.09	0.017±0.002	T268	15200±3800	5.9±0.9	0.07±0.01
Q198	5600±1800	1.00±0.09	0.017±0.003	E272	17400±4700	6± 1	0.07±0.02
E200	7900±1300	1.44±0.08	0.024±0.002	I283	14200±2100	7.2±0.6	0.072±0.008
W202	4070± 840	2.4±0.1	0.023±0.002	M285	14700±4100	5.0±0.8	0.06±0.01
F203	7490± 770	11.1±0.4	0.066±0.004	Q286	18600±6400	27± 6	0.16±0.04
E204	9290± 850	3.4±0.1	0.040±0.002	Y292	2160± 630	3.2±0.1	0.019±0.002
K205	5830± 270	11.8±0.2	0.060±0.001	R294	6200±1500	1.9±0.1	0.025±0.003
A206	4080± 950	2.0±0.1	0.020±0.002	V296	14100±2400	6.9±0.7	0.071±0.009
L207	7600±1200	4.0±0.2	0.039±0.004	Q300	6670± 570	2.68±0.07	0.030±0.001
R208	4980± 940	2.9±0.1	0.027±0.002	Y301	10260± 810	21.0±0.7	0.106±0.005
K210	7500±2300	1.6±0.2	0.025±0.004	S302	4570± 990	2.2±0.1	0.023±0.002
K211	3030± 950	3.7±0.2	0.024±0.003	E309	5760± 700	2.6±0.09	0.028±0.002
F213	5800±1700	1.6±0.1	0.022±0.003	I311	9900±1200	7.6±0.4	0.062±0.005
I215	7200±1200	1.69±0.09	0.025±0.002	N312	7400±1400	2.8±0.2	0.033±0.003
K219	12900±2500	2.2±0.2	0.038±0.005	H315	10440± 920	1.02±0.04	0.024±0.001
E220	8900±1500	1.34±0.09	0.025±0.002	G316	18200±2000	5.8±0.4	0.074±0.007
D221	6900±2200	1.1±0.1	0.020±0.003	I317	7210± 900	3.5±0.1	0.036±0.002
A223	6000±1700	1.9±0.2	0.024±0.003	E323	9800±1600	1.01±0.07	0.023±0.002
C224	8500±1900	3.2±0.3	0.038±0.005	S328	6000±1400	2.0±0.1	0.025±0.003
L225	15200±3300	4.4±0.6	0.059±0.009	Y329	5880± 290	12.4±0.2	0.061±0.002
F226	12300±4100	3.5±0.6	0.05±0.01	R331	7880± 890	38± 2	0.125±0.008
R227	14100±3000	4.5±0.5	0.057±0.009	N336	6300±1400	1.9±0.1	0.025±0.003
D231	7500±2400	1.9±0.2	0.027±0.005	S337	8500±2600	1.6±0.2	0.026±0.005
Y234	3990± 670	5.0±0.2	0.032±0.002				
D238	6400±1600	2.0±0.2	0.026±0.003				
M239	8900±2200	2.1±0.2	0.031±0.004				
H246	4600±1500	1.7±0.1	0.02±0.003				
C247	7800±2700	1.4±0.2	0.024±0.005				
N254	6100±1200	2.1±0.1	0.026±0.003				
A255	13000±1900	8.6±0.7	0.076±0.008				
Y257	9500±1400	3.1±0.2	0.039±0.004				
F258	5470± 850	3.4±0.1	0.031±0.002				
S259	9200±1100	4.4±0.2	0.046±0.003				
N260	13700±2900	11± 1	0.09±0.01				
Y261	12000±2500	4.0±0.4	0.05±0.007				
V262	7960 ±960	6.5±0.3	0.052±0.004				

* Only residues that display <35% uncertainty in k_{ex} and R_{ex} > 1.0 s^{-1} are shown.

References:

[1] Wiener, R., Zhang, X., Wang, T., and Wolberger, C. (2012) The mechanism of OTUB1-mediated inhibition of ubiquitination, *Nature 483*, 618-622.

[2] Madeira, F., Park, Y. M., Lee, J., Buso, N., Gur, T., Madhusoodanan, N., Basutkar, P., Tivey, A. R. N., Potter, S. C., Finn, R. D., and Lopez, R. (2019) The EMBL-EBI search and sequence analysis tools APIs in 2019, *Nucleic Acids Res. 47*, W636-W641.

[3] Robert, X., and Gouet, P. (2014) Deciphering key features in protein structures with the new ENDscript server, *Nucleic Acids Res. 42*, W320-324.

[4] Shen, Y., and Bax, A. (2013) Protein backbone and sidechain torsion angles predicted from NMR chemical shifts using artificial neural networks, *J. Biomol. NMR 56*, 227-241.